

Indole-3-acetamides: As Potential Antihyperglycemic and Antioxidant Agents; Synthesis, *In Vitro* α -Amylase Inhibitory Activity, Structure–Activity Relationship, and *In Silico* Studies

Kanwal, Khalid Mohammed Khan,* Sridevi Chigurupati, Farman Ali, Munissa Younus, Maha Aldubayan, Abdul Wadood, Huma Khan, Muhammad Taha, and Shahnaz Perveen



Cite This: ACS Omega 2021, 6, 2264–2275



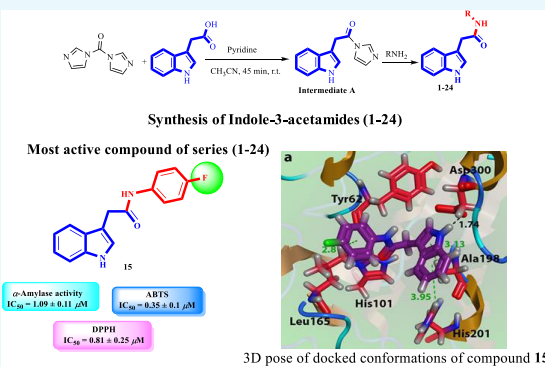
Read Online

ACCESS |

Metrics & More

Article Recommendations

ABSTRACT: Indole-3-acetamides (**1–24**) were synthesized via coupling of indole-3-acetic acid with various substituted anilines in the presence of coupling reagent 1,1-carbonyldiimidazole. The structures of synthetic molecules were elucidated through different spectroscopic techniques including electron ionization-mass spectroscopy (EI-MS), ^1H -, ^{13}C NMR, and high-resolution EI-MS (HREI-MS). These compounds were screened for their antihyperglycemic and antioxidant potentials. All compounds displayed good to moderate inhibition against α -amylase enzyme with IC_{50} values ranging between 1.09 ± 0.11 and $2.84 \pm 0.1 \mu\text{M}$ compared to the standard acarbose ($\text{IC}_{50} = 0.92 \pm 0.4 \mu\text{M}$). Compound **15** ($\text{IC}_{50} = 1.09 \pm 0.11 \mu\text{M}$) was the most active compound of the series and exhibited good inhibition against α -amylase; in addition, this compound also exhibited good antioxidant potential with IC_{50} values of 0.35 ± 0.1 and $0.81 \pm 0.25 \mu\text{M}$ in 2,2-diphenyl-1-picryl-hydrazyl-hydrate (DPPH) and 2,2'-azino-bis(3-ethylbenzothiazoline-6-sulfonic acid) (ABTS) assays, respectively. The binding interactions of synthetic molecules with the enzyme's active site were confirmed via *in silico* studies. The current study had identified a number of lead molecules as potential antihyperglycemic and antioxidant agents.



INTRODUCTION:

Diabetes mellitus (DM), one of the common metabolic disorders, is usually characterized by irregular blood glucose levels. The elevated level of blood glucose is referred to as hyperglycemia, which results due to the abnormal functionality of enzyme insulin. Insulin is a peptide hormone that is secreted through the islets of Langerhans. Any damage to these cells leads to either less or no secretion of insulin, which consequently leads to uncontrolled levels of glucose in blood.^{1–3} There are many pathways through which diabetes can be controlled, one of which is enzyme inhibition. Since digestive enzymes such as α -amylase have been known to increase blood glucose, one of the methods to control diabetes is the inhibition of this enzyme for controlled digestion of carbohydrates in diabetic patients.⁴ α -Amylase is an enzyme (EC.3.2.1.1) that hydrolyzes α -1,4 glycoside bonds of complex carbohydrate molecules such as starch and glycogen to yield glucose and maltose. It contains calcium in its active site and is found in normal serum, saliva, and urine of humans. It is also found in bacteria and other living organisms. Primarily, α -amylase hydrolyzes complex carbohydrate molecules into small oligosaccharides and maltodextrins, and by the action of another digestive enzyme α -glucosidase, they are finally converted to glucose and absorbed in the bloodstream.⁵

Therefore, inhibition of α -amylase would be an ideal therapy to control diabetes and its related complications.⁶ Prolonged diabetes mainly affects the metabolism of proteins, fats, carbohydrates, water, and electrolytes and thus leads to various structural changes in tissues of vital organ systems in the body, especially the vascular system.⁷ The increased level of blood glucose prompts several metabolic signaling pathways that leads to inflammation, cytokines secretion, cell death, and subsequently diabetic complications.⁸ Therefore, diabetic patients are commonly found to be associated with damage of heart, kidney, skin, eye, foot, etc. Alzheimer's disease, a common neurological disorder, is also associated with prolonged effects of this disease.⁷ The high prevalence and rapid increase of diabetes have attracted the attention of many researchers, and hence many drugs have been developed for its control and cure. However, to date, no drug has been able to

Received: November 16, 2020

Accepted: December 31, 2020

Published: January 12, 2021



completely cure this disease. Commercially available α -amylase inhibitors are associated with a number of side effects, most commonly gastrointestinal complications. Therefore, there is still a need and space for the development of cheap and less harmful drugs that can be easily available having potent antidiabetic activity.^{9,10}

Among many complications associated with DM, the formation of reactive oxygen species (ROS) is also common and leads to severe damage of many vital organs. A number of free radicals and reactive oxygen species are formed during metabolism, and using antioxidants, these free radicals are neutralized without any harmful effect to our body. Free radicals may harm our immune system by a number of degenerative ailments. Free radicals are chemically unstable species with unpaired electrons. These unpaired electrons capture electrons from neighboring biomolecules like DNA, proteins, and lipids, thus initiating chain reactions in the body, which triggers the abnormal behavior of these biomolecules.^{11–13} Mitochondrial respiratory chain enzymes, *e.g.*, xanthine oxidase, lipoxygenase, etc., affect the production of ROS due to hyperglycemia.¹⁶ Thus, a high level of ROS and oxidative stress in diabetes leads to cellular death through numerous mechanisms that finally leads to tissue damage.^{17–19} Therefore, diabetic complications can be controlled through the downregulation of ROS generation.^{20–22}

Indole belongs to the class of heterocyclic compounds and possesses a benzene ring fused with a pyrrole ring with a 10-electron system from four double bonds and one nitrogen atom lone pair. It has been used as a primary precursor molecule for the synthesis of a variety of pharmaceuticals and fragrances.^{23,24} Indomethacin and strychnine are among the most common biologically active synthetic and natural product resources that are derived from indole.²⁵ Indole and its related compounds possess a wide range of biological activities and are part of many medicinally important nuclei, which were widely accepted as pharmacophores.²⁶ Currently, indole nucleus has been found to be a part of more than 200 compounds that are marked as drugs or are undergoing clinical trials.²⁷ Indoles are an important class of compounds in the field of medicinal chemistry and found to have different biological activities including anticancer, anti-inflammatory, antiulcerogenic, antibacterial, antiviral, antifungal, etc.^{28–31} Previously, our research group had explored and reported the potential antihyperglycemic activity of different indole derivatives.^{32–35} Keeping in mind the antidiabetic potential of indoles, the synthetic molecules were considered for their α -amylase inhibition and antioxidant activity. The results showed that these compounds have dual abilities of lowering the postprandial hyperglycemia and scavenging the free radicals effectively and may serve as lead molecules in drug discovery and development (Figures 1 and 2). To the best of our knowledge, compounds 1, 6, 8, and 13 are reported in the literature and the remaining compounds are new.

RESULTS AND DISCUSSION

Chemistry. Indole-3-acetamides (1–24) were synthesized via a one-pot multicomponent reaction of indole-3-acetic acid with 1,1-carbonyldiimidazole (CDI) and different substituted anilines.³⁶ First, indole-3-acetic acid was allowed to react with CDI in the presence of catalytic amount of pyridine in acetonitrile. Pyridine used in this reaction helps in the deprotonation of carboxylic acid and makes it more feasible to react with the coupling reagent. CO₂ gas evolved during the

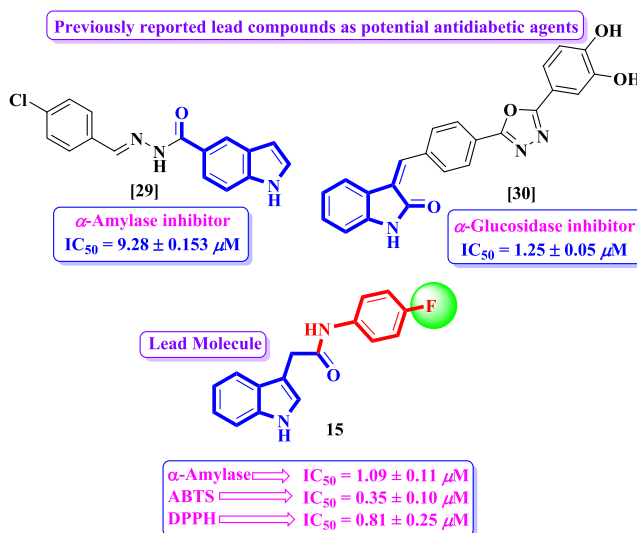


Figure 1. Rationale of the current study.

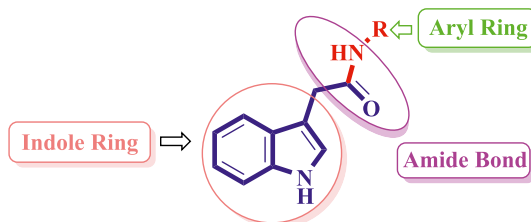


Figure 2. General structure of synthetic compounds (1–24).

reaction resulted in the formation of an intermediate A, which was subsequently treated with different substituted anilines to afford indole-3-acetamides. The synthetic analogues were purified and characterized using different spectroscopic techniques including ¹H-, ¹³C NMR, electron ionization-mass spectroscopy (EI-MS), and high-resolution EI-MS (HREI-MS) (Table 1).

In Vitro α -Amylase Inhibitory Activity and DPPH and ABTS Radical Scavenging Activities. Twenty-four indole-3-acetamides 1–24 were synthesized and screened for antihyperglycemic and antioxidant activities. The molecules 1–24 displayed good to moderate inhibition against α -amylase enzyme with IC_{50} values ranging between 1.09 ± 0.11 and $2.84 \pm 0.1 \mu M$. However, the antioxidant potential was evaluated with DPPH and ABTS radical scavenging activities. All synthetic derivatives potentially scavenged the reactive oxygen species in the IC_{50} value ranges of 0.35 ± 0.1 – 2.19 ± 0.08 and 0.81 ± 0.25 – $2.75 \pm 0.03 \mu M$ for ABTS and DPPH activities, respectively (Scheme 1).

Structure–Activity Relationship for α -Amylase Inhibition. Limited structure–activity relationship suggested that compound 1 ($IC_{50} = 2.6 \pm 0.09 \mu M$) bearing unsubstituted phenyl ring demonstrated moderate inhibition against α -amylase enzyme in comparison to the standard acarbose ($IC_{50} = 0.92 \pm 0.4 \mu M$). The addition of methyl group at the *para* position of phenyl ring resulted in slightly reduced activity in compound 2 ($IC_{50} = 2.84 \pm 0.1 \mu M$). Compounds 3, 4, and 5 with dimethyl substitutions at different positions of aryl ring displayed variable inhibitory activity. Among them, compound 3 ($IC_{50} = 2.52 \pm 0.06 \mu M$) with *meta*- and *para*-substituted methyl groups was moderately active. Changing the position of the methyl group from *meta* to *ortho* resulted in decreased

Table 1. *In Vitro* α -Amylase Inhibitory, DPPH, and ABTS Radical Scavenging Activities of Compounds 1–24

Comp. No.	R	α -Amylase IC ₅₀ ± SEM ^a (μ M)	ABTS IC ₅₀ ± SEM ^a (μ M)	DPPH IC ₅₀ ± SEM ^a (μ M)
1		2.60 ± 0.09	1.77 ± 0.1	2.36 ± 0.2
2		2.84 ± 0.1	2.19 ± 0.08	2.75 ± 0.03
3		2.52 ± 0.06	1.58 ± 0.11	2.22 ± 0.09
4		2.68 ± 0.08	1.90 ± 0.1	2.67 ± 0.12
5		2.38 ± 0.1	1.36 ± 0.15	1.79 ± 0.19
6		2.42 ± 0.07	1.38 ± 0.26	1.92 ± 0.08
7		2.43 ± 0.1	1.45 ± 0.15	2.02 ± 0.12
8		2.15 ± 0.1	0.99 ± 0.33	1.04 ± 0.1
9		2.42 ± 0.1	1.43 ± 0.3	2.00 ± 0.07
10		2.24 ± 0.06	1.11 ± 0.1	1.53 ± 0.1
11		2.63 ± 0.1	1.78 ± 0.2	2.42 ± 0.1
12		2.64 ± 0.1	1.80 ± 0.1	2.45 ± 0.04
13		2.10 ± 0.1	0.58 ± 0.4	1.03 ± 0.3
14		2.27 ± 0.04	1.14 ± 0.2	1.59 ± 0.11
15		1.09 ± 0.11	0.35 ± 0.1	0.81 ± 0.25
16		2.25 ± 0.05	1.12 ± 0.2	1.53 ± 0.13
17		2.38 ± 0.05	1.31 ± 0.1	1.71 ± 0.12
18		2.2 ± 0.08	1.08 ± 0.2	1.42 ± 0.18
19		2.28 ± 0.08	1.15 ± 0.2	1.61 ± 0.11
20		2.14 ± 0.08	0.66 ± 0.2	1.04 ± 0.14
21		1.76 ± 0.2	0.46 ± 0.19	0.97 ± 0.19
22		2.33 ± 0.09	1.28 ± 0.2	1.62 ± 0.15
23		2.48 ± 0.06	1.52 ± 0.1	2.22 ± 0.07
24		2.15 ± 0.09	0.94 ± 0.2	0.80 ± 0.14
Acarbose ^(Std)		0.92 ± 0.4		
Ascorbic Acid ^(Std)			0.23 ± 0.14	0.51 ± 0.18

^aSEM is the standard error of the mean, Acarbose^(std) is the standard inhibitor for α -amylase inhibitory activity, and Ascorbic acid^(std) is the standard inhibitor for 2,2-diphenyl-1-picryl-hydrazyl-hydrate (DPPH) and 2,2'-azino-bis(3-ethylbenzothiazoline-6-sulfonic acid) (ABTS) activity.

Scheme 1. Synthesis of Indole-3-acetamides (1–24)

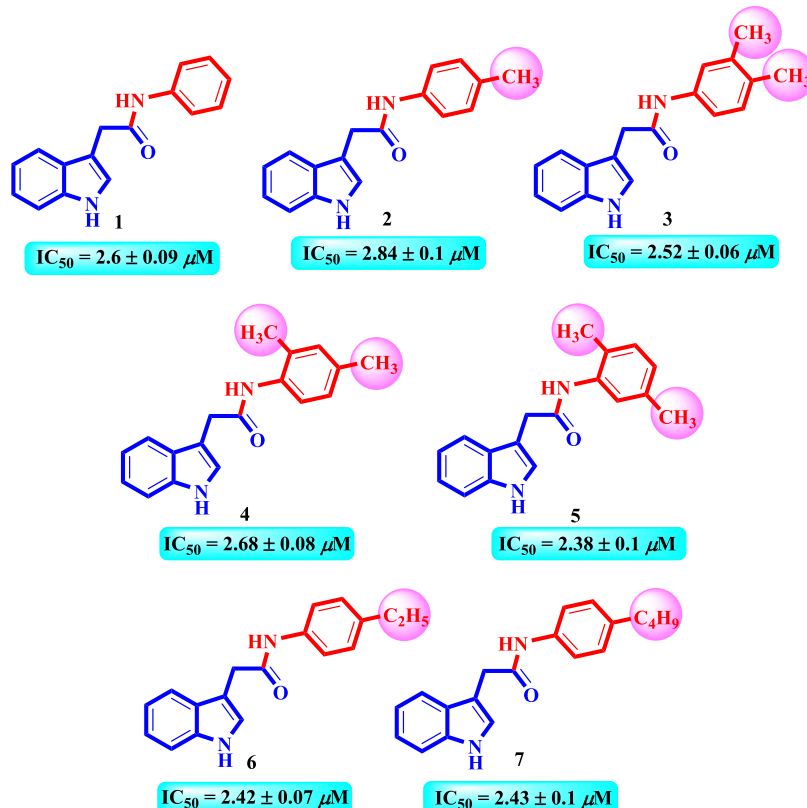
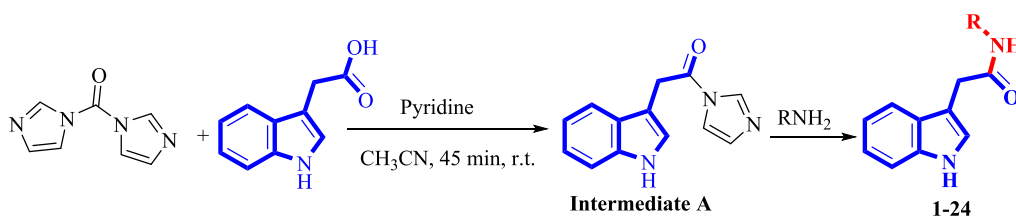


Figure 3. SAR of alkyl-substituted compounds 1–7.

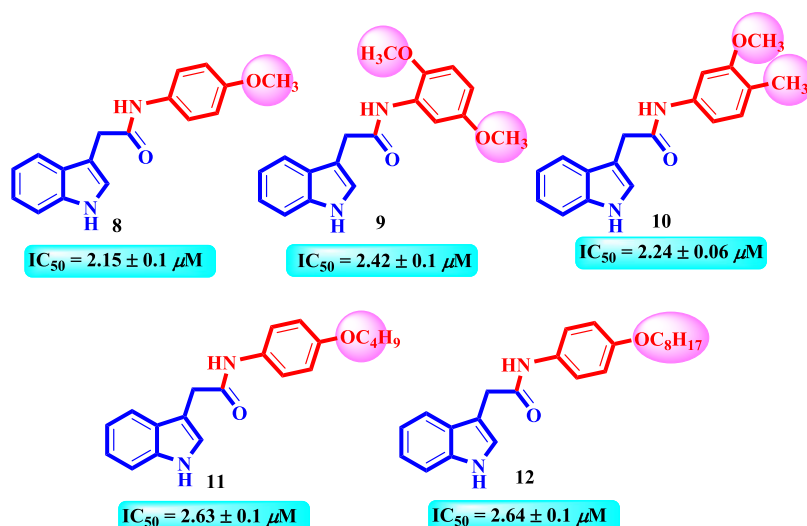


Figure 4. SAR of alkoxy-substituted compounds 8–12.

inhibitory activity in compound 4 (IC₅₀ = 2.68 ± 0.08 μM). Nevertheless, compound 5 (IC₅₀ = 2.38 ± 0.1 μM) with

methyl groups para to each other showed superior activity among methyl-substituted compounds. Thus, compounds with

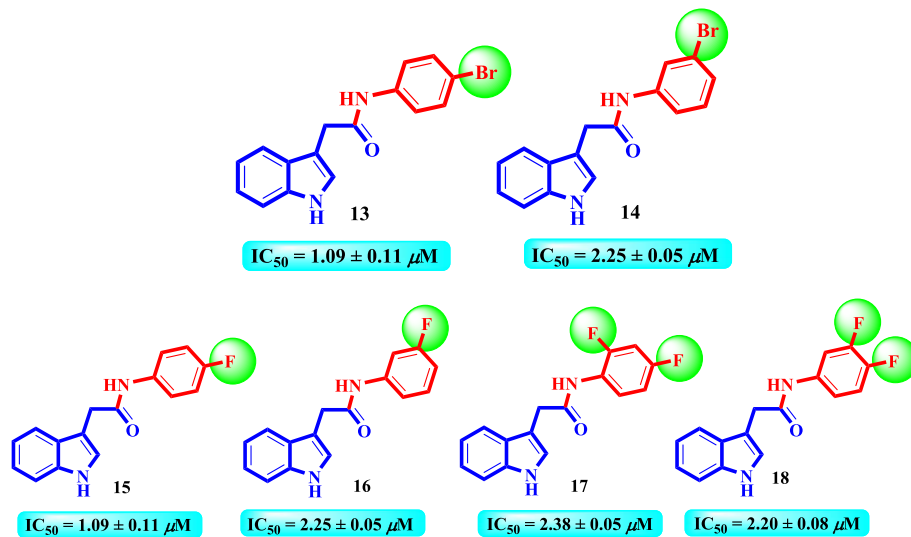


Figure 5. SAR of halogen-substituted compounds 13–18.

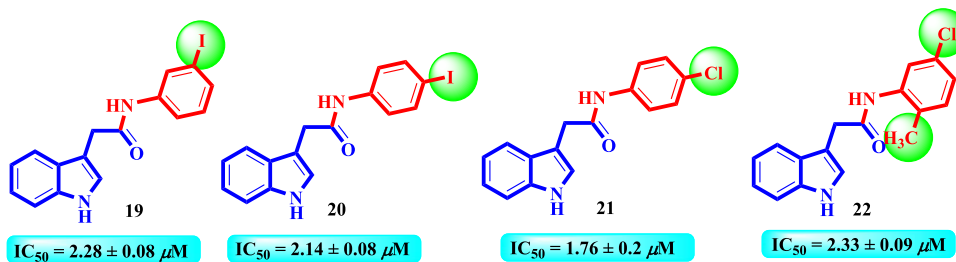


Figure 6. SAR of halogen-substituted compounds 19–22.

dimethyl substitution were more active in comparison to mono methyl- and unsubstituted compounds 1 and 2, which might be due to the better interaction of methyl groups within the active site of enzyme. Nevertheless, compounds 6 ($IC_{50} = 2.42 \pm 0.07 \mu M$) and 7 ($IC_{50} = 2.43 \pm 0.1 \mu M$) with *para*-substituted ethyl and butyl groups, respectively, have shown similar activity (Figure 3).

Compound 8 ($IC_{50} = 2.15 \pm 0.1 \mu M$) bearing *para* methoxy substituents displayed superior activity to methyl-substituted derivatives. Compound 9 ($IC_{50} = 2.42 \pm 0.07 \mu M$) having two methoxy groups *para* to each other resulted in slightly decreased inhibition. Replacing one of the methoxy groups with methyl and changing their position in compound 10 ($IC_{50} = 2.24 \pm 0.06 \mu M$) resulted in better inhibition compared to compound 9. Interestingly, compound 11 ($IC_{50} = 2.63 \pm 0.1 \mu M$) having *para*-substituted butoxy group displayed similar activity to compound 12 ($IC_{50} = 2.64 \pm 0.1 \mu M$) with octyloxy substitution (Figure 4).

Among halogen-substituted derivatives, compound 13 ($IC_{50} = 2.1 \pm 0.1 \mu M$) bearing bromo group at *para* substitution was slightly more active in comparison to the *meta* bromo-substituted compound 14 ($IC_{50} = 2.27 \pm 0.04 \mu M$). Compound 15 ($IC_{50} = 1.09 \pm 0.11 \mu M$) having *para* fluoro group was the most active compound of this series, which may be due to the inductive effect of the fluoro group. Changing the position of the fluoro group from *para* to *meta* in compound 16 ($IC_{50} = 2.25 \pm 0.05 \mu M$) resulted in decreased inhibition. Nonetheless, compound 17 ($IC_{50} = 2.38 \pm 0.05 \mu M$) with two fluoro atoms at *ortho* and *para* positions, respectively, demonstrated moderate inhibition in comparison to the

standard acarbose, which was also found to be less active than compound 15, which showed that addition of another fluoro atom resulted in increased inductive effect, thus making it less available to bind with the active site of enzyme. Compound 18 ($IC_{50} = 2.20 \pm 0.08 \mu M$) with changed positions of the fluoro group also displayed similar activity to compound 17 (Figure 5).

Compound 19 ($IC_{50} = 2.28 \pm 0.08 \mu M$) having a *meta*-substituted iodo group was less active compared with the *para* iodo-substituted compound 20 ($IC_{50} = 2.14 \pm 0.08 \mu M$). Compound 21 ($IC_{50} = 1.76 \pm 0.2 \mu M$) with *para* chloro substitution was the second most active compound of the series. Compound 22 ($IC_{50} = 2.33 \pm 0.09 \mu M$) bearing chloro and methyl substituents *para* to each other displayed weak inhibition in comparison to compound 21. The decreased activity of this compound might be due to the addition of methyl group and change in the position of the chloro group (Figure 6).

Compounds 23 ($IC_{50} = 2.48 \pm 0.06 \mu M$) and 24 ($IC_{50} = 2.15 \pm 0.09 \mu M$) with *meta* and *para* thiomethyl groups, respectively, also displayed weak inhibition against α -amylase in comparison to standard acarbose ($IC_{50} = 0.92 \pm 0.4 \mu M$) (Figure 7).

ABTS and DPPH Radical Scavenging Activities and Structure–Activity Relationships. Among 24 synthetic derivatives, the *para* flouro-substituted compound 15 was found to exhibit superior ABTS and DPPH radical scavenging activities in comparison to *para* chloro-, bromo-, and iodo-substituted compounds 21, 13, and 20, respectively. It showed that the flouro group with a high negative inductive effect and

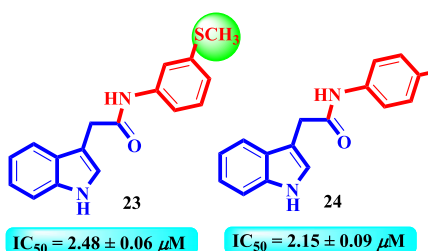


Figure 7. SAR of thiomethyl-substituted compounds 23–24.

the smallest size among all halogen substituents was most active, and an increased size of halogen atoms and decreased inductive effect resulted in declined scavenging activity. Compounds 14, 16, and 19 with *meta* bromo, flouro, and iodo substituents, respectively, displayed similar activities; nonetheless, these compounds were less active in comparison to their *para*-substituted analogues. Compounds 17 and 18 bearing di-flouro substituents at *ortho* para and *meta* para positions, respectively, also displayed decreased activity in comparison to mono flouro-substituted compound 15. This pattern showed that the number, nature, and positions of the halogen groups play a crucial role in DPPH and ABTS radical scavenging activities.

The methyl-substituted derivative 2 displayed weak antioxidant activity; nonetheless, the dimethyl-substituted compounds 3, 4, and 5 showed superior activity in comparison to compound 2, which might be due to the addition of another methyl group that resulted in better activity due to the hyperconjugation effect. Compounds 6 and 7 with ethyl and butyl groups, respectively, also displayed comparable activities to methyl-substituted compounds. Compound 8 bearing a methoxy group displayed better activity than methyl-substituted compounds. However, dimethoxy-substituted

compound 9 was less active than compound 8. The general activity pattern revealed that compounds with halogen substitutions were better antioxidant agents compared to methyl and methoxy.

Hyperglycemia has many adverse effects along with the promotion of auto-oxidation of glucose to form free radicals. The antioxidant defense system is capable of scavenging a particular amount of free radicals; thus, the excessive production of free radicals results in macro- and microvascular dysfunction and polyneuropathy. Therefore, the drugs that can effectively scavenge the free-radical formation would be a preferable therapeutic strategy to prevent oxidative stress and the related diabetic vascular complications. Since the synthetic molecules (1–24) were capable of inhibiting the activity of α -amylase enzyme as well as free radicals, these molecules might act as lead candidates for drug discovery and research. Further research and modifications in the structures of these molecules might be helpful for the discovery of new drug molecules.

Molecular Docking study. *In silico* docking simulation was conducted to explore the binding modes of indole-3-acetamide derivatives 1–24 against α -amylase enzyme. The crystal structure of α -amylase (PDB ID: 1HNY) was downloaded from Protein Data Bank for docking study. Docking simulation was performed by MOE-2016 software. Using the default parameters of MOE, the α -amylase enzyme and the newly synthesized compounds were protonated and energy-minimized to get the optimized structures of the protein and compounds. These optimized structures of target protein and compounds were further used for docking studies.

Docking Results Analysis. The docking study was used to explore the binding interactions of the ligand molecules into α -amylase active-site residues. At the end of docking simulation, the binding interactions of all of the 24 compounds were discussed and their 3D images were taken. From the docking

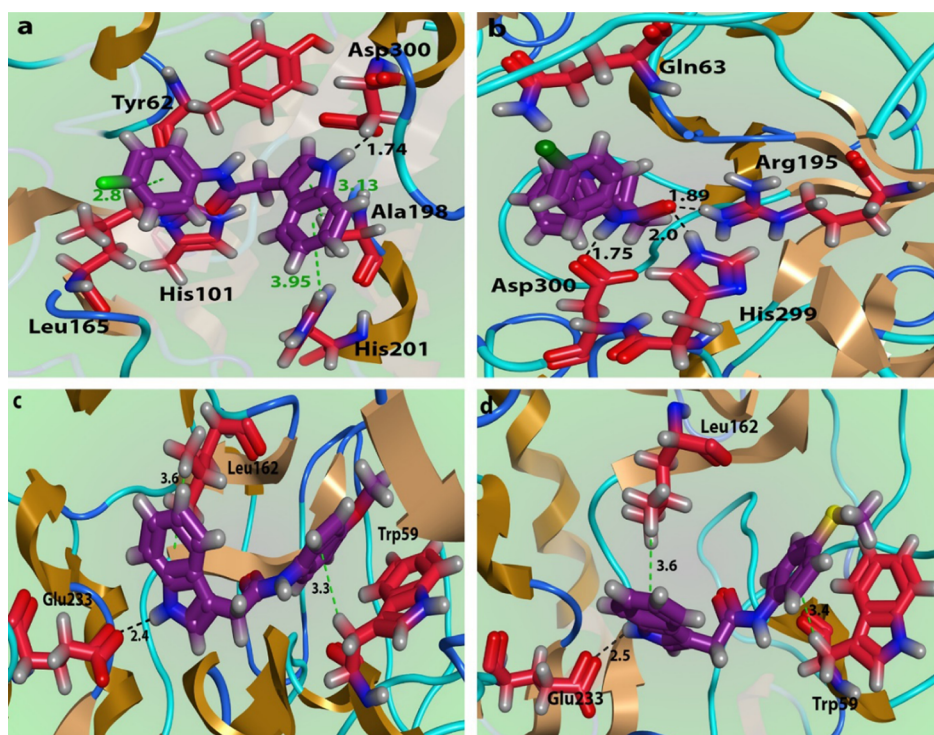


Figure 8. 3D pose of docked conformations of compounds 15 (a), 21 (b), 8 (c), and 24 (d) (purple) in the active site of α -amylase enzyme (red).

Table 2. Interaction Details, Docking Score Binding Energy, and Binding Affinity of the Compound Docked in the Active Site of α -Amylase Enzyme

C. no.	docking score	binding energy (kcal/mol)	binding affinity (kcal/mol)	interaction detail (ligands/ α -amylase)	C. no.	docking score	binding energy (kcal/mol)	binding affinity (kcal/mol)	interaction detail (ligands/ α -amylase)
1	-5.548	25.16	-5.29	ligand–receptor interaction distance N 11 OD1 ASP 300 H-donor 3.00 N 11 OD2 ASP 300 H-donor 3.24	12				N 11 OE2 GLU 240 H-donor 3.08
2	-5.777	-27.14	-5.66	ligand–receptor interaction distance N 11 OD2 ASP 300 H-donor 2.94	13	-5.135	-29.03	-5.80	ligand–receptor interaction distance N 11 OD1 ASP 197 H-donor 2.91
3	-5.466	-26.78	-5.30	ligand–receptor@@ interaction distance N 11 OD1 ASP 300 H-donor 3.05 6-ring 5-ring TRP 59 pi-pi 3.58 6-ring 6-ring TRP 59 pi-pi 3.99	14	-5.212	-28.85	-5.99	BR 33 OD2 ASP 356 H-donor 3.2 ligand–receptor interaction distance O 22 CE1 HIS 201 H-acceptor 3.23
4	-5.767	-27.90	-5.61	ligand–receptor interaction distance N 11 OD1 ASP 300 H-donor 2.97 N 11 OD2 ASP 300 H-donor 3.26	15	-5.625	-27.84	-5.61	ligand–receptor interaction distance N 11 OD2 ASP 300 H-donor 1.74 6-ring CD2 LEU 165 pi-H 2.8 5-ring CB ALA 198 pi-H 3.13 6-ring CE1 HIS 201 pi-H 3.95
5	-5.814	-28.06	-5.62	ligand–receptor interaction distance N 11 OD1 ASP 300 H-donor 3.05 N 11 OD2 ASP 300 H-donor 3.00	16	-5.444	-27.69	-5.73	ligand–receptor interaction distance N 11 OD1 ASP 197 H-donor 2.99
6	-5.165	-29.75	-5.81	ligand–receptor interaction distance N 11 OD1 ASP 197 (A) H-donor 3.02 5-ring CB ALA 198 (A) pi-H 4.67	17	-5.35	-25.44	-5.06	6-ring CD1 LEU 162 pi-H 4.79 ligand–receptor interaction distance N 11 OD1 ASP 300 H-donor 3.08
7	-5.468	-30.35	-6.15	ligand–receptor interaction distance 5-ring CB TYR 62 pi-H 4.04	18	-5.066	-31.00	-5.78	N 20 OD1 ASP 300 H-donor 3.09
8	-5.6	-34.41	-5.98	ligand–receptor interaction distance N 11 OE1 GLU 233 H-donor 2.4 6-ring CB TRP 59 pi-H 3.3	19	-5.331	-28.92	-5.81	6-ring CD1 LEU 162 pi-H 3.6 ligand–receptor interaction distance I 33 OD2 ASP 356 H-donor 3.91
9	-5.685	-26.76	-5.41	ligand–receptor interaction distance N 11 OD1 ASP 300 (A) H-donor 3.10	20	-5.221	-31.46	-5.89	5-ring CB ALA 198 pi-H 4.70 ligand–receptor interaction distance N 20 OD1 ASP 300 H-donor 2.89
10	-5.296	-35.44	-6.28	ligand–receptor interaction distance N 20 OD1 ASP 300 H-donor 3.18	21	-5.6	-32.31	-5.99	N 20 OD1 ASP 300 H-donor 1.75 ligand–receptor interaction distance O 22 NH2 ARG 195 H-acceptor 1.89
11	-6.48	-33.37	-6.32	ligand–receptor interaction distance N 11 OD1 ASP 300 H-donor 3.04	22	-5.807	-32.81	-6.40	O 22 NE2 HIS 299 H-acceptor 2.00 ligand–receptor interaction distance N 20 OD1 ASP 300 H-donor 3.02
12	-6.756	-38.25	-6.92	ligand–receptor interaction distance N 11 OD2 ASP 300 H-donor 3.11 C 13 6-ring TYR 62 H-pi 4.22	23	-5.683	-26.56	-5.48	6-ring 5-ring TRP 59 pi-pi 3.71 ligand–receptor interaction distance N 11 OD2 ASP 300 H-donor 3.07
					24	-5.658	-32.99	-5.75	C 13 6-ring TYR 62 H-pi 4.15 ligand–receptor interaction distance N 11 OE1 GLU 233 H-donor 2.5
									6-ring CB TRP 59 pi-H 3.4 6-ring CD1 LEU 162 pi-H 3.6

study, it was revealed that the docked conformations of all of the compounds are appropriately oriented toward the catalytic residues, making sufficient interactions with the active-site residues Trp58, Trp59, Tyr62, Leu162, Arg195, Asp197, Glu233, Asp300, and His305 of the target enzyme.

Interactions of the Halides Containing Compounds. Compounds 13–22 are grouped as halide-containing compounds. All of these compounds have the same 2-(1*H*-indol-3-yl)-*N*-phenylacetamide group, whereas the phenyl ring contains different halide groups. According to the IC₅₀ value, compound 15 ($1.09 \pm 0.11 \mu\text{M}$) is the most active compound of this group. It is clear from Figure 8a that compound 15 was bound deeply into the binding cavity of α -amylase showing four interactions with the residues Leu165, Ala198, His201, and Asp300. The hydrogen bond was observed between Asp300 and the indole moiety of compound 15, whereas the aromatic rings of the compound show π –H interactions with the Leu165, Ala198, and His201 residues of the protein.

Compound 21 is the second most active compound (IC₅₀ = $1.76 \pm 0.2 \mu\text{M}$) in this group, forming three prominent hydrogen bonds with the binding-site residues Arg195, His299, and Asp300, as shown in Figure 8b.

The key structural feature observed in this group for good interaction mode and active nature of compounds is the presence of an electron-withdrawing group like halogen groups at specific positions on the phenyl ring.

Interactions of the Alkoxy- and Methanethiol-Containing Compounds. To discuss the interaction details, compounds 8–12 were placed in the second group due to the presence of the alkoxy group on the phenyl ring. Compound 8 is the most active compound (IC₅₀ = $2.15 \pm 0.1 \mu\text{M}$) in this group that shows hydrogen bonding with Glu233 and π –H interactions with Trp59 and Leu162, as shown in Figure 8c.

However, compounds 23 and 24 have a common methanethiol group on the phenyl ring with different *meta* and *para* positions. Compound 11 was observed in making good interactions with active-site residues Glu233, Trp59, and leu162 (Figure 8d). Compound 23 shows higher activity (IC₅₀ = $2.15 \pm 0.09 \mu\text{M}$) than compound 24. It may due to the *para* position of the methanethiol group, which is the activating group.

Interactions of the Alkyl-Containing Compounds. Compounds 1–7 contain alkyl groups on the phenol moiety of the acetamide core structure at various ortho, meta, and para positions. Compound 22 of this group containing chloromethylphenyl group shows the best activity (IC₅₀ = $2.33 \pm 0.09 \mu\text{M}$) against α -amylase enzyme. The NH group of the indole moiety of the compound makes a hydrogen bond with Asp300, and the phenol ring shows π – π interaction with Trp59 active-site residues. The activity may be due to the presence of chloro-methylphenyl moiety Table 2.

Overall, the whole series of 2-(1*H*-indol-3-yl)-*N*-phenylacetamide derivatives shows the best activity against α -amylase enzyme. Different groups like halides, methanethiol, alkyl, and alkoxy groups at various positions of the phenol ring of the phenylacetamide compound may be responsible for their best inhibitory activity against α -amylase enzyme. Details about the interaction and docking of these compounds are given in Table 2.

CONCLUSIONS

Indole-3-acetamides (1–24) were synthesized and evaluated for α -amylase inhibition along with antioxidant activity. All

synthetic compounds displayed good inhibition against α -amylase. The synthetic molecules are also found to have good antioxidant potential. Among 24 derivatives, compounds 6, 11, 15, and 18 were found to exhibit potential inhibition compared to the standard acarbose (IC₅₀ = $0.92 \pm 0.40 \mu\text{M}$). The molecular docking studies identified the types of binding interactions, which helped the synthetic compounds to interact within the active site of enzyme. Thus, this study identified many lead candidates that can act as potential antidiabetic and antioxidant agents.

EXPERIMENTAL SECTION

Materials and Methods. Thin-layer chromatography (TLC) was carried out on precoated silica gel, GF-254 (Merck, Germany). Spots were visualized under ultraviolet light at 254 and 366 nm. EI-MS and HREI-MS spectra were recorded on MAT 312 and MAT 113D mass spectrometers. ¹H and ¹³C NMR spectra were recorded on a Bruker Avance AM spectrometer operating at 300 MHz. The chemical shift values are presented in ppm (δ), relative to tetramethylsilane (TMS) as an internal standard, and the coupling constants (J) are in hertz. The melting points of the compounds were determined on a Stuart SMP10 melting point apparatus and are uncorrected.

General Procedure for the Synthesis of Indole-3-acetamides (1–24). Indole-3-acetic acid (0.175 g, 1 mmol), pyridine (0.8 mL), and CDI 1 equivalent (0.168 g) were taken in a reaction flask along with acetonitrile (20 mL) and stirred for 45 min at room temperature. The corresponding anilines were then added to the reaction mixture, and the mixture was continuously stirred for 2–24 h. The reaction was monitored with TLC, and the products were obtained by extraction with dichloromethane. The product was then washed with hexane to get pure product.³⁶

α -Amylase Inhibition Assay. The activity was performed through modified assay from Kwon, Apostolidis, and Shetty.^{37,38} Phosphate buffer (0.2 mM, pH 6.9) in 500 μL of α -amylase solution obtained from *Aspergillus oryzae* (0.5 mg/mL) was incubated with 500 μL of test sample (100, 200, 400, 800, 1000 μg/mL) at 25 °C for 10 min. Sodium phosphate buffer (0.02 M, pH 6.9) with 1% starch solution (500 μL) was added to each tube and further incubated for 10 min at 25 °C. The reaction mixture was then incubated in boiling water for 5 min after addition of 1 mL of dinitrosalicylic acid. The reaction mixture was then cooled to room temperature. The absorbance was measured at 540 nm after the addition of 10 mL of distilled water. The percentage inhibition was calculated as illustrated

$$\begin{aligned} \% \text{ inhibition} &= (\text{absorbance}_{\text{control}} - \text{absorbance}_{\text{sample}}) \\ &/ \text{absorbance}_{\text{control}} \times 100 \end{aligned}$$

Molecular Docking Studies. *In silico* docking simulation was conducted to explore the binding modes of indole-3-acetamide derivatives against α -amylase enzyme. The crystal structure of α -amylase (PDB ID: 1HNY) was downloaded from Protein Data Bank for docking study. Docking simulation was performed by MOE-2016 software. Using the default parameters of MOE, the α -amylase enzyme and the newly synthesized compounds were protonated and energy-minimized to get the optimized structures of the protein and compounds. These optimized structures of target protein and compounds were further used for docking studies.³⁹

Spectral Data of Synthetic Compounds (1–24). 2-(1*H*-Indol-3-yl)-*N*-phenylacetamide (**1**). Yield: 78%; mp: 186–188 °C; ¹H NMR (300 MHz, acetone-*d*₆): δ 10.14 (s, 1H, NH), 9.04 (s, 1H, NH), 7.62 (m, 3H, H-4', H-2', H-6'), 7.38 (d, *J*_{4,5} = 8.1 Hz, 1H, H-4), 7.32 (s, 1H, H2), 7.24 (t, *J* = 8.4 Hz, 2H, H-3', H-5'), 7.11 (m, 1H, H-6), 7.03 (m, 2H, H-5, H-7), 3.80 (s, 2H, H-2''); ¹³C NMR (300 MHz, dimethyl sulfoxide (DMSO)-*d*₆): δ 169.6, 139.3, 136.0, 128.6, 127.1, 123.8, 122.9, 120.9, 119.0, 118.6, 118.3, 111.3, 108.5, 33.7; EI-MS *m/z* (% rel. abund.): 250 (M⁺, 82.6), 157 (22), 130 (100), 103 (57), 93 (54), 77 (70); HREI-MS *m/z*: calcd for C₁₆H₁₄N₂O [250.1106], found [250.1095].

2-(1*H*-Indol-3-yl)-*N*-(*p*-tolyl) acetamide (**2**). Yield: 21%; mp: 187–188 °C; ¹H NMR (300 MHz, acetone-*d*₆): δ 10.12 (s, 1H, NH), 8.94 (s, 1H, NH), 7.64 (d, *J* = 7.8 Hz, 1H, H-4), 7.47 (d, *J* = 8.4 Hz, 2H, H-2', H-6'), 7.38 (d, *J* = 7.8 Hz, 1H, H-7), 7.31 (s, 1H, H-2), 7.04 (m, 4H, H-3', H-5', H-5, H-6), 3.78 (s, 2H, H-2''), 2.22 (s, 3H, CH₃); ¹³C NMR (300 MHz, DMSO-*d*₆): δ 169.4, 136.8, 136.0, 131.8, 128.9, 127.2, 123.7, 120.9, 119.0, 118.6, 118.3, 111.3, 108.6, 33.7, 20.3; EI-MS *m/z* (% rel. abund.): 264 (M⁺, 80), 131 (53), 130 (100).

N-(3,4-Dimethylphenyl)-2-(1*H*-indol-3-yl)acetamide (**3**). Yield: 89%; mp: 158–160 °C; ¹H NMR (300 MHz, acetone-*d*₆): δ 10.12 (s, 1H, NH), 8.82 (s, 1H, NH), 7.63 (d, *J* = 8.1 Hz, 1H, H-4), 7.36 (m, 4H, H-5', H-6', H-2, H-7), 7.10 (t, *J* = 7.2 Hz, 1H, H-5), 7.01 (m, 2H, H-6, H-2'), 3.77 (s, 2H, H-2''), 2.14 (s, 6H, CH₃); ¹³C NMR (300 MHz, DMSO-*d*₆): δ 169.3, 137.0, 136.1, 136.0, 130.6, 129.4, 127.1, 123.7, 120.9, 120.3, 118.6, 118.3, 116.5, 111.2, 108.6, 33.7, 19.5, 18.6; EI-MS *m/z* (% rel. abund.): 278 (M⁺, 57), 131 (34), 130 (100), 121 (25); HREI-MS *m/z*: calcd for C₁₈H₁₈N₂O [278.1419], found [278.1431].

N-(2,4-Dimethylphenyl)-2-(1*H*-indol-3-yl)acetamide (**4**). Yield: 51%; mp: 142–144 °C; ¹H NMR (300 MHz, acetone-*d*₆): δ 10.22 (s, 1H, NH), 8.22 (s, 1H, NH), 7.68 (d, *J* = 7.8 Hz, 1H, H-4), 7.44 (m, 3H, H-2, H-5', H-7), 7.12 (t, *J* = 7.8 Hz, 1H, H-5), 7.01 (m, 2H, H-6, H-3'), 6.90 (d, *J* = 7.2 Hz, 1H, H-6'), 3.84 (s, 2H, H-2''), 2.82 (s, 3H, CH₃), 1.84 (s, 3H, CH₃); ¹³C NMR (300 MHz, DMSO-*d*₆): δ 169.6, 136.7, 136.2, 136.1, 130.8, 127.1, 126.6, 125.0, 123.8, 123.2, 120.9, 118.6, 118.3, 111.3, 108.7, 38.3, 38.1, 33.0; EI-MS *m/z* (% rel. abund.): 278 (M⁺, 93), 131 (52), 130 (100), 121 (25); HREI-MS *m/z*: calcd for C₁₈H₁₈N₂O [278.1419], found [278.1422].

N-(2,5-Dimethylphenyl)-2-(1*H*-indol-3-yl)acetamide (**5**). Yield: 53%; mp: 151–153 °C; ¹H NMR (300 MHz, acetone-*d*₆): δ 10.24 (s, 1H, NH), 8.08 (s, 1H, NH), 7.65 (m, 2H, H-6', H-2), 7.42 (d, *J* = 6.3 Hz, 2H, H-7, H-4), 7.12 (t, *J* = 7.2 Hz, 1H, H-5), 7.04 (t, *J* = 7.5 Hz, 1H, H-6), 6.94 (d, *J* = 7.5 Hz, 1H, H-3'), 6.78 (d, *J* = 7.5 Hz, 1H, H-4'), 3.84 (s, 2H, H-2''), 2.23 (s, 3H, CH₃), 1.85 (s, 3H, CH₃); ¹³C NMR (300 MHz, DMSO-*d*₆): δ 169.4, 136.2, 136.1, 134.8, 129.9, 128.0, 127.1, 125.5, 125.1, 123.8, 120.9, 118.5, 118.3, 111.3, 108.7, 33.1, 20.5, 17.1; EI-MS *m/z* (% rel. abund.): 278 (M⁺, 58), 131 (22), 130 (100), 121 (11); HREI-MS *m/z*: calcd for C₁₈H₁₈N₂O [278.1419], found [278.1408].

N-(4-Ethylphenyl)-2-(1*H*-indol-3-yl)acetamide (**6**). Yield: 42%; mp: 160–162 °C; ¹H NMR (300 MHz, acetone-*d*₆): δ 10.11 (s, 1H, NH), 8.93 (s, 1H, NH), 7.63 (d, *J* = 7.8 Hz, 1H, H-4), 7.50 (d, *J* = 8.4 Hz, 2H, H-2', H-6'), 7.38 (d, *J* = 7.8 Hz, 1H, H-7), 7.32 (s, 1H, H-2), 7.08 (m, 3H, H-3', H-5', H-5), 7.01 (t, *J* = 7.5 Hz, 1H, H-6), 3.78 (s, 2H, H-2''), 2.54 (m, 2H, CH₂), 1.15 (t, *J* = 7.5 Hz, 3H, CH₃); ¹³C NMR (300 MHz, DMSO-*d*₆): δ 169.4, 138.3, 137.0, 136.0, 127.8, 127.1, 123.7,

120.9, 119.1, 118.6, 118.3, 111.3, 108.6, 33.7, 27.5, 15.6; EI-MS *m/z* (% rel. abund.): 278 (M⁺, 33), 157 (5), 130 (100); HREI-MS *m/z*: calcd for C₁₈H₁₈N₂O [278.1419], found [278.1400].

N-(4-Butylphenyl)-2-(1*H*-indol-3-yl)acetamide (**7**). Yield: 97%; mp: 141–143 °C; ¹H NMR (300 MHz, acetone-*d*₆): δ 10.13 (s, 1H, NH), 8.95 (s, 1H, NH), 7.63 (d, *J* = 7.5 Hz, 1H, H-4), 7.50 (d, *J* = 8.7 Hz, 2H, H-2', H-6'), 7.38 (d, *J* = 8.1 Hz, 1H, H-7), 7.32 (s, 1H, H-2), 7.06 (m, 4H, H-5, H-6, H-3', H-5'), 3.78 (s, 2H, H-2''), 2.53 (t, *J* = 7.5 Hz, 2H, CH₂), 1.52 (m, 2H, CH₂), 1.29 (m, 2H, CH₂), 0.88 (t, *J* = 7.5 Hz, 3H, CH₃); ¹³C NMR (300 MHz, DMSO-*d*₆): δ 169.4, 137.0, 136.9, 136.0, 128.3, 127.1, 123.7, 120.9, 119.0, 118.6, 118.3, 111.3, 108.6, 34.1, 33.7, 33.1, 21.6, 13.7; EI-MS *m/z* (% rel. abund.): 306 (M⁺, 86), 130 (100), 106 (33); HREI-MS *m/z*: calcd for C₂₀H₂₂N₂O [306.1732], found [306.1699].

2-(1*H*-Indol-3-yl)-*N*-(4-methoxyphenyl)acetamide (**8**). Yield: 81%; M.p.: 184–185 °C; ¹H NMR (300 MHz, Acetone-*d*₆): δ 10.12 (s, 1H, NH), 8.88 (s, 1H, NH), 7.64 (d, *J* = 7.8 Hz, 1H, H-4), 7.50 (d, *J* = 9.0 Hz, 2H, H-2', H-6'), 7.38 (d, *J* = 7.8 Hz, 1H, H-7), 7.31 (s, 1H, H-2), 7.10 (t, *J* = 7.5 Hz, 1H, H-5), 7.00 (t, *J* = 7.2 Hz, 1H, H-6), 6.80 (d, *J* = 9.0 Hz, 2H, H-3', H-5'), 3.76 (s, 2H, H-2''), 3.72 (s, 3H, OCH₃); ¹³C NMR (300 MHz, DMSO-*d*₆): δ 169.1, 155.0, 136.0, 132.5, 127.2, 123.7, 120.9, 120.5, 118.6, 118.3, 113.7, 111.3, 108.6, 55.1, 33.6; EI-MS *m/z* (% rel. abund.): 280 (M⁺, 27), 130 (100), 108 (10); HREI-MS *m/z*: calcd for C₁₇H₁₆N₂O₂ [280.1212], found [280.1194].

N-(2,5-Dimethoxyphenyl)-2-(1*H*-indol-3-yl)acetamide (**9**). Yield: 35%; mp: 152–154 °C; ¹H NMR (300 MHz, acetone-*d*₆): δ 10.27 (s, 1H, NH), 8.37 (s, 1H, NH), 8.08 (d, *J* = 3 Hz, 1H, H-6'), 7.63 (d, *J* = 8.1 Hz, 1H, H-3'), 7.45 (s, 1H, H-2), 7.42 (m, 1H, H-4), 7.16 (m, 1H, H-5), 7.05 (m, 1H, H-6), 6.77 (d, *J* = 8.7 Hz, 1H, H-7), 6.48 (dd, *J*_{4',6'} = 3 Hz, *J*_{4',3'} = 3 Hz, 1H, H-4'), 3.87 (s, 2H, H-2''), 3.69 (s, 3H, OCH₃), 3.49 (s, 3H, OCH₃); ¹³C NMR (300 MHz, acetone-*d*₆): δ 170.1, 154.7, 143.1, 137.8, 130.0, 128.2, 125.2, 122.5, 1119.9, 119.4, 112.3, 112.1, 109.4, 107.7, 106.7; EI-MS *m/z* (% rel. abund.): 310 (M⁺, 61), 153 (24), 138 (25), 130 (100); HREI-MS *m/z*: calcd for C₁₈H₁₈N₂O₃ [310.1317], found [310.1314].

2-(1*H*-Indol-3-yl)-*N*-(3-methoxy-4-methylphenyl)acetamide (**10**). Yield: 33%; mp: 102–104 °C; ¹H NMR (300 MHz, acetone-*d*₆): δ 10.12 (s, 1H, NH), 8.95 (s, 1H, NH), 7.64 (d, *J* = 7.8 Hz, 1H, H-4), 7.38 (d, *J* = 7.5 Hz, 2H, H-7, H-6'), 7.32 (s, 1H, H-2), 7.11 (t, *J* = 7.2 Hz, 1H, H-5), 7.02 (m, 3H, H-2', H-5', H-6), 3.78 (s, 2H, H-2''), 3.73 (s, 3H, OCH₃), 2.04 (m, 3H, CH₃); ¹³C NMR (300 MHz, DMSO-*d*₆): δ 169.5, 157.1, 138.5, 136.0, 130.0, 127.2, 123.8, 120.9, 119.9, 118.6, 118.3, 111.3, 110.5, 108.5, 101.8, 54.9, 33.8, 15.5; EI-MS *m/z* (% rel. abund.): 294 (M⁺, 34), 157 (5), 130 (100), 77 (8); HREI-MS *m/z*: calcd for C₁₈H₁₈N₂O₂ [294.1368], found [294.1381].

N-(4-Butoxyphenyl)-2-(1*H*-indol-3-yl)acetamide (**11**). Yield: 77%; mp: 174–177 °C; ¹H NMR (300 MHz, acetone-*d*₆): δ 10.11 (s, 1H, NH), 8.85 (s, 1H, NH), 7.64 (d, *J* = 7.8 Hz, 1H, H-4), 7.49 (d, *J* = 9.0 Hz, 2H, H-2', H-6'), 7.38 (d, *J* = 8.1 Hz, 1H, H-7), 7.31 (s, 1H, H-2), 7.10 (t, *J* = 7.2 Hz, 1H, H-5), 7.01 (t, *J* = 7.5 Hz, 1H, H-6), 6.80 (d, *J* = 9.0 Hz, 2H, H-3', H-5'), 3.91 (t, *J* = 6.3 Hz, 2H, OCH₂), 3.76 (s, 2H, CH₂), 1.71 (m, 2H, CH₂), 1.45 (m, 2H, CH₂), 0.92 (t, *J* = 7.5 Hz, 3H, CH₃); EI-MS *m/z* (% rel. abund.): 322 (M⁺, 96), 131 (60), 130 (100), 109 (54); HREI-MS *m/z*: calcd for C₂₀H₂₂N₂O₂ [322.1681], found [322.1703].

2-(1H-Indol-3-yl)-N-(4-(octyloxy) phenyl)acetamide (12). Yield: 79%; M.p.: 155–157 °C, ¹H NMR (300 MHz, acetone-*d*₆): δ 10.12 (s, 1H, NH), 8.87 (s, 1H, NH), 7.63 (d, *J* = 7.8 Hz 1H, H-4), 7.49 (d, *J* = 8.1 Hz, 2H, H-2', H-6'), 7.38 (d, *J* = 8.1 Hz, 1H, H-7), 7.31 (s, 1H, H-2), 7.10 (t, *J* = 7.5 Hz, 1H, H-5), 7.00 (t, *J* = 7.5 Hz, 1H, H-6), 6.79 (d, *J* = 9.0 Hz, 2H, H-3', H-5'), 3.91 (t, *J* = 6.6 Hz, 2H, OCH₂), 3.76 (s, 2H, H-2''), 1.71 (m, 2H, CH₂), 1.41 (m, 2H, CH₂), 1.29 (m, 8H, CH₂, CH₂, CH₂, CH₂), 0.85 (m, 3H, CH₃); EI-MS *m/z* (% rel. abund.): 378 (M⁺, 74), 131 (71), 130 (100), 109 (65), HREI-MS *m/z*: calcd for C₁₆H₁₃BrN₂O [328.0211], found [328.0233].

N-(4-Bromophenyl)-2-(1H-indol-3-yl)acetamide (13). Yield: 62%; mp: 196–198 °C, ¹H NMR (300 MHz, acetone-*d*₆): δ 10.14 (s, 1H, NH), 9.19 (s, 1H, NH), 7.60 (m, 3H, H-4, H-3', H-5'), 7.41 (m, 3H, H-2', H-6', H-7), 7.32 (s, 1H, H-2), 7.08 (m, 1H, H-5), 7.01 (m, 1H, H-6), 3.80 (s, 2H, H-2''); ¹³C NMR (300 MHz, DMSO-*d*₆): δ 205.9, 170.4, 139.6, 132.2, 128.3, 124.6, 122.1, 121.7, 119.6, 119.3, 115.7, 112.0, 109.4, 34.9; EI-MS *m/z* (% rel. abund.): 328 (M⁺, 39), 330 (M⁺², 7), 130 (100), 103 (11.2), 77 (9); HREI-MS *m/z*: calcd for C₁₆H₁₃BrN₂O [328.0211], found [328.0202].

N-(3-Bromophenyl)-2-(1H-indol-3-yl)acetamide (14). Yield: 58%; mp: 133–135 °C, ¹H NMR (300 MHz, acetone-*d*₆): δ 10.14 (s, 1H, NH), 9.22 (s, 1H, NH), 8.03 (s, 1H, H-2'), 7.62 (d, *J* = 7.8 Hz, 1H, H-4'), 7.49 (m, 1H, H-6'), 7.38 (d, *J* = 8.1 Hz, 1H, H-7), 7.32 (s, 1H, H-2), 7.19 (m, 2H, H-4, H-5'), 7.10 (t, *J* = 7.8 Hz, 1H, H-5), 7.01 (t, *J* = 8.1 Hz, 1H, H-6), 3.81 (s, 2H, H-2''); ¹³C NMR (300 MHz, DMSO-*d*₆): δ 170.0, 140.9, 136.0, 130.6, 127.1, 125.5, 123.8, 121.4, 121.3, 120.9, 118.5, 118.3, 117.7, 111.3, 108.1, 33.7; EI-MS *m/z* (% rel. abund.): 328 (M⁺, 56), 330 (M⁺², 9), 130 (100), 103 (17); HREI-MS *m/z*: calcd for C₁₆H₁₃BrN₂O [328.0211], found [328.0233].

N-(4-Fluorophenyl)-2-(1H-indol-3-yl)acetamide (15). Yield: 76%; mp: 108–110 °C, ¹H NMR (300 MHz, acetone-*d*₆): δ 10.14 (s, 1H, NH), 9.29 (s, 1H, NH), 7.69 (m, 1H, H-3'), 7.64 (m, 1H, H-5'), 7.39 (d, *J* = 8.5 Hz, 1H, H-4), 7.32 (s, 1H, H-2), 7.69 (m, 2H, H-2', H-6'), 7.12 (m, 1H, H-5), 7.02 (m, 1H, H-6), 6.77 (m, 1H, H-7), 3.78 (s, 2H, H-2''); ¹³C NMR (300 MHz, DMSO-*d*₆): δ 169.5, 157.1, 138.5, 136.0, 130.0, 127.2, 123.8, 120.9, 119.9, 118.6, 118.3, 111.3, 110.5, 108.5, 101.8, 54.9, 33.8, 15.5; EI-MS *m/z* (% rel. abund.): 268 (M⁺, 68), 157 (2), 130 (100); HREI-MS *m/z*: calcd for C₁₆H₁₃FN₂O [268.1012], found [268.1003].

N-(3-Fluorophenyl)-2-(1H-indol-3-yl)acetamide (16). Yield: 91%; mp: 148–150 °C, ¹H NMR (300 MHz, acetone-*d*₆): δ 10.13 (s, 1H, NH), 9.10 (s, 1H, NH), 7.61 (m, 3H, H-2', H-4', H-4), 7.38 (d, *J* = 8.1 Hz, 1H, H-7), 7.31 (s, 1H, H-2), 7.09 (t, *J* = 7.8 Hz, 1H, H-5), 7.02 (m, 3H, H-6, H-5', H-6'), 3.79 (s, 2H, H-2''); EI-MS *m/z* (% rel. abund.): 268 (M⁺, 100), 157 (7), 130 (100); HREI-MS *m/z*: calcd for C₁₆H₁₃FN₂O [268.1012], found [268.1022].

N-(2,4-Difluorophenyl)-2-(1H-indol-3-yl)acetamide (17). Yield: 72%; mp: 133–135 °C, ¹H NMR (300 MHz, acetone-*d*₆): δ 10.19 (s, 1H, NH), 8.69 (s, 1H, NH), 8.14 (m, 1H, H-5'), 7.64 (d, *J* = 7.8 Hz, 1H, H-6'), 7.38 (m, 2H, H-2, H-4), 7.10 (t, *J* = 7.5 Hz, 1H, H-5), 7.04 (m, 1H, H-6), 6.95 (m, 2H, H-3', H-7), 3.89 (s, 2H, H-2''); ¹³C NMR (300 MHz, DMSO-*d*₆): δ 170.0, 136.0, 127.1, 125.6, 130.0, 127.2, 123.8, 120.9, 119.9, 118.6, 118.3, 111.3, 110.5, 108.5, 101.8, 54.9, 33.8, 15.5; EI-MS *m/z* (% rel. abund.): 286 (M⁺, 17), 130 (100), 77 (18); HREI-MS *m/z*: calcd for C₁₆H₁₂FN₂O [286.0918], found [286.0912].

N-(3,4-Difluorophenyl)-2-(1H-indol-3-yl)acetamide (18). Yield: 78%; mp: 100–102 °C, ¹H NMR (300 MHz, acetone-*d*₆): δ 10.15 (s, 1H, NH), 9.30 (s, 1H, NH), 7.84 (m, 1H, H-5'), 7.62 (d, *J* = 7.8 Hz, 1H, H-4), 7.38 (d, *J* = 8.1 Hz, 1H, H-7), 7.31 (s, 1H, H-2), 7.24 (m, 1H, H-2'), 7.18 (m, 1H, H-6'), 7.14 (m, 1H, H-5), 7.01 (t, *J* = 7.8 Hz, 1H, H-6), 3.80 (s, 2H, H-2''); EI-MS *m/z* (% rel. abund.): 286 (M⁺, 92), 131 (63), 130 (100); HREI-MS *m/z*: calcd for C₁₆H₁₂F₂N₂O [286.0918], found [286.0943].

2-(1H-Indol-3-yl)-N-(3-iodophenyl)acetamide (19). Yield: 64%; mp: 136–138 °C, ¹H NMR (300 MHz, acetone-*d*₆): δ 10.13 (s, 1H, NH), 9.15 (s, 1H, NH), 8.18 (s, 1H, H-2'), 7.63 (d, *J* = 7.8 Hz, 1H, H-4'), 7.54 (d, *J* = 7.5 Hz, 1H, H-6'), 7.38 (d, *J* = 7.8 Hz, 1H, H-4), 7.32 (s, 1H, H-2), 7.07 (m, 4H, H-5', H-5, H-6, H-7), 3.81 (s, 2H, H-2''); EI-MS *m/z* (% rel. abund.): 376 (M⁺, 95), 131 (42), 130 (100), HREI-MS *m/z*: calcd for C₁₆H₁₃IN₂O [376.0073], found [376.0032].

2-(1H-Indol-3-yl)-N-(4-iodophenyl)acetamide (20). Yield: 16%; mp: 211–213 °C, ¹H NMR (300 MHz, acetone-*d*₆): δ 10.13 (s, 1H, NH), 9.16 (s, 1H, NH), 7.60 (m, 3H, H-6', H-2', H-4), 7.46 (d, *J* = 9.0 Hz, 2H, H-3', H-5'), 7.39 (d, *J* = 8.1 Hz, 1H, H-7), 7.31 (s, 1H, H-2), 7.09 (t, *J* = 7.5 Hz, 1H, H-5), 7.01 (t, *J* = 7.5 Hz, 1H, H-6), 3.80 (s, 2H, H-2''); EI-MS *m/z* (% rel. abund.): 376 (M⁺, 10), 218 (3), 130 (100); HREI-MS *m/z*: calcd for C₁₆H₁₃IN₂O [376.0073], found [376.0052].

N-(4-Chlorophenyl)-2-(1H-indol-3-yl)acetamide (21). Yield: 56%; mp: 161–163 °C, ¹H NMR (300 MHz, acetone-*d*₆): δ 10.13 (s, 1H, NH), 9.18 (s, 1H, NH), 7.64 (m, 3H, H-5', H-3', H-4), 7.38 (d, *J* = 8.1 Hz, 1H, H-7), 7.32 (s, 1H, H-2), 7.25 (d, *J* = 9.0 Hz, 2H, H-2', H-6'), 7.10 (t, *J* = 7.2 Hz, 1H, H-5), 7.02 (t, *J* = 7.5 Hz, 1H, H-6), 3.80 (s, 2H, H-2''); ¹³C NMR (300 MHz, DMSO-*d*₆): δ 169.8, 138.3, 136.1, 128.5, 127.2, 126.5, 123.9, 121.0, 120.6, 118.6, 118.4, 111.4, 108.3, 33.8; EI-MS *m/z* (% rel. abund.): 283 (M⁺, 16), 285 (M⁺², 4), 130 (100), 77 (23); HREI-MS *m/z*: calcd for C₁₆H₁₃ClN₂O [284.0716], found [284.0724].

N-(5-Chloro-2-methylphenyl)-2-(1H-indol-3-yl)acetamide (22). Yield: 13%; mp: 201–203 °C, ¹H NMR (300 MHz, acetone-*d*₆): δ 10.26 (s, 1H, NH), 8.20 (s, 1H, NH), 8.01 (s, 1H, H-6'), 7.64 (d, *J* = 7.8 Hz, 1H, H-4'), 7.43 (m, 2H, H-4, H-2), 7.10 (m, 3H, H-5, H-6, H-3'), 6.98 (m, 1H, H-7), 3.88 (s, 2H, H-2''), 1.88 (s, 3H, CH₃); ¹³C NMR (300 MHz, DMSO-*d*₆): δ 169.9, 137.7, 136.1, 131.6, 129.7, 129.4, 127.1, 124.2, 124.0, 123.4, 121.0, 118.5, 118.4, 111.3, 108.5, 33.1, 17.1; EI-MS *m/z* (% rel. abund.): 298 (M⁺, 7), 300 (M⁺², 2), 130 (100), 76 (S6); HREI-MS *m/z*: calcd for C₁₇H₁₅ClN₂O [298.0873], found [298.0873].

2-(1H-Indol-3-yl)-N-(3-(methylthio) phenyl)acetamide (23). Yield: 71%; mp: 123–125 °C, ¹H NMR (300 MHz, acetone-*d*₆): δ 10.13 (s, 1H, NH), 9.06 (s, 1H, NH), 7.66 (m, 1H, H-6'), 7.63 (d, *J* = 8.1 Hz, 1H, H-4), 7.38 (d, *J* = 8.7 Hz, 1H, H-7), 7.35 (s, 1H, H-2), 7.31 (m, 1H, H-2'), 7.18 (t, *J* = 8.1 Hz, 1H, H-5'), 7.07 (m, 1H, H-5), 7.01 (m, 1H, H-6), 6.91 (m, 1H, H-4'), 3.80 (s, 2H, H-2''), 2.42 (s, 3H, SCH₃); ¹³C NMR (300 MHz, DMSO-*d*₆): δ 169.5, 157.1, 138.5, 136.0, 130.0, 127.2, 123.8, 120.9, 119.9, 118.6, 118.3, 111.3, 110.5, 108.5, 101.8, 54.9, 33.8, 15.5; EI-MS *m/z* (% rel. abund.): 296 (M⁺, 9), 130 (100), 77 (28); HREI-MS *m/z*: calcd for C₁₇H₁₆N₂OS [296.0983], found [296.0970].

2-(1H-Indol-3-yl)-N-(4-(methylthio) phenyl)acetamide (24). Yield: 86%; mp: 184–186 °C, ¹H NMR (300 MHz, acetone-*d*₆): δ 10.12 (s, 1H, NH), 9.05 (s, 1H, NH), 7.63 (d, *J* = 7.8 Hz, 1H, H-4), 7.58 (d, *J* = 8.7 Hz, 2H, H-2', H-6'),

7.38(d, $J = 8.1$ Hz, 1H, H-7), 7.31 (s, 1H, H-2), 7.18(m, 2H, H-3', H-5'), 7.07 (m, 1H, H-5), 7.01 (m, 1H, H-6), 3.79 (s, 2H, H-2''), 2.42 (s, 3H, SCH₃); EI-MS m/z (% rel. abund.): 296 (M⁺, 11), 130 (100), 77 (27); HREI-MS m/z : calcd for C₁₇H₁₆N₂OS [296.0983], found [296.0976].

AUTHOR INFORMATION

Corresponding Author

Khalid Mohammed Khan – *H. E. J. Research Institute of Chemistry, International Center for Chemical and Biological Sciences, University of Karachi, Karachi 75270, Pakistan; Department of Clinical Pharmacy, Institute for Research and Medical Consultations (IRMC), Imam Abdulrahman Bin Faisal University, Dammam 31441, Saudi Arabia;* orcid.org/0000-0001-8337-4021; Phone: 0092-21-34824910; Email: khalid.khan@iccs.edu, drkhalidhej@gmail.com; Fax: 0092-21-34819018

Authors

Kanwal – *H. E. J. Research Institute of Chemistry, International Center for Chemical and Biological Sciences, University of Karachi, Karachi 75270, Pakistan; Institute of Marine Biotechnology, Universiti Malaysia Terengganu, 21030 Kuala Terengganu, Terengganu, Malaysia*

Sridevi Chigurupati – *Department of Medicinal Chemistry and Pharmacognosy, College of Pharmacy, Qassim University, Buraidah 52571, Saudi Arabia*

Farman Ali – *H. E. J. Research Institute of Chemistry, International Center for Chemical and Biological Sciences, University of Karachi, Karachi 75270, Pakistan*

Munissa Younus – *H. E. J. Research Institute of Chemistry, International Center for Chemical and Biological Sciences, University of Karachi, Karachi 75270, Pakistan*

Maha Aldubayan – *Department of Pharmacology and Toxicology, College of Pharmacy, Qassim University, Buraidah 52571, Saudi Arabia*

Abdul Wadood – *Department of Biochemistry, Computational Medicinal Chemistry Laboratory, UCSS, Abdul Wali Khan University, Mardan 23200, Pakistan*

Huma Khan – *Department of Biochemistry, Computational Medicinal Chemistry Laboratory, UCSS, Abdul Wali Khan University, Mardan 23200, Pakistan*

Muhammad Taha – *Department of Clinical Pharmacy, Institute for Research and Medical Consultations (IRMC), Imam Abdulrahman Bin Faisal University, Dammam 31441, Saudi Arabia*

Shahnaz Perveen – *PCSIR Laboratories Complex, Karachi, Karachi 75280, Pakistan*

Complete contact information is available at:

<https://pubs.acs.org/10.1021/acsomegajournal/0c05581>

Notes

The authors declare no competing financial interest.

ACKNOWLEDGMENTS

The authors are thankful to the Pakistan Academy of Sciences, Pakistan, for providing financial support to Project No. (S-9/PAS/440).

REFERENCES

- (1) Piero, M. N.; Nzaro, G. M.; Njagi, J. M. Diabetes mellitus—a devastating metabolic disorder. *Asian J. Biomed. Pharm. Sci.* **2014**, 4, 1–7.
- (2) Adeghate, E. Diabetes mellitus-multifactorial in aetiology and global in prevalence. *Arch. Physiol. Biochem.* **2001**, 109, 197–199.
- (3) Adeghate, E.; Schattner, P.; Dunn, E. An update on the etiology and epidemiology of diabetes mellitus. *Ann. NY Acad. Sci.* **2006**, 1084, 1–29.
- (4) Alam, F.; Shafique, Z.; Amjad, S. T.; Bin Asad, M. H. H. Enzymes inhibitors from natural sources with antidiabetic activity: A review. *Phytother. Res.* **2019**, 33, 41–54.
- (5) Tiwari, S. P.; Srivastava, R.; Singh, C. S.; Shukla, K.; Singh, R. K.; Singh, P.; Singh, R.; Singh, N. L.; Sharma, R. Amylases: An overview with special reference to α -amylase. *J. Glob. Biosci.* **2015**, 4, 1886–1901.
- (6) Agarwal, P.; Gupta, R. α -Amylase inhibition can treat diabetes mellitus. *Res. Rev. J. Med. Heal. Sci.* **2016**, 5, 1–9.
- (7) Lee, H. J.; Seo, H. I.; Cha, H. Y.; Yang, Y. J.; Kwon, S. H.; Yang, S. J. Diabetes and Alzheimer's disease: mechanisms and nutritional aspects. *Clin. Nutr. Res.* **2018**, 7, 229–240.
- (8) Esposito, K.; Nappo, F.; Marfella, R.; Giugliano, G.; Giugliano, F.; Cirotola, M.; Giugliano, D.; et al. Inflammatory cytokine concentrations are acutely increased by hyperglycemia in humans: role of oxidative stress. *Circulation* **2002**, 106, 2067–2072.
- (9) Tundis, R.; Loizzo, M. R.; Menichini, F. Natural products as α -amylase and α -glucosidase inhibitors and their hypoglycemic potential in the treatment of diabetes: An update. *Mini-Rev. Med. Chem.* **2010**, 10, 315–331.
- (10) Nair, S. S.; Kavrekar, V.; Mishra, A. *In vitro* studies on α -amylase and α -glucosidase inhibitory activities of selected plant extracts. *Eur. J. Exp. Biol.* **2013**, 3, 128–132.
- (11) Chen, N.; Karantza-Wadsworth, V. Role and regulation of autophagy in cancer. *Biochim. Biophys. Acta* **2009**, 1793, 1516–1523.
- (12) Gonzalez, C. D.; Lee, Myung-Shik; Marchetti, P.; Pietropaolo, M.; Towns, R.; Vaccaro, M. I.; Watada, H.; Wiley, J. W. The emerging role of autophagy in the pathophysiology of diabetes mellitus. *Autophagy* **2011**, 7, 2–11.
- (13) Hara, T.; Nakamura, K.; Matsui, M.; Yamamoto, A.; Nakahara, Y.; Suzuki-Migishima, R.; Yokoyama, M.; Mishima, K.; Saito, I.; Okano, H.; Mizushima, N. Suppression of basal autophagy in neural cells causes neurodegenerative disease in mice. *Nature* **2006**, 441, 885–889.
- (14) Krakauer, T. Inflammasome, mTORC1 activation, and metabolic derangement contribute to the susceptibility of diabetics to infections. *Med. Hypotheses* **2015**, 85, 997–1001.
- (15) Zhang, Y.; Peng, T.; Zhu, H.; Zheng, X.; Zhang, X.; Jiang, N.; Cheng, X.; Lai, X.; Shunnar, A.; Singh, M.; Riordan, N.; Bogin, V.; Tong, N.; Min, W. P. Prevention of hyperglycemia-induced myocardial apoptosis by gene silencing of Toll-like receptor-4. *J. Transl. Med.* **2010**, 8, No. 133.
- (16) Bajaj, S.; Khan, A. Antioxidants and diabetes. *Indian J. Endocrinol. Metab.* **2012**, 16, S267–S271.
- (17) Khan, K. M.; Khan, A.; Taha, M.; Salar, U.; Hameed, A.; Ismail, N. H.; Jamil, W.; Saad, S. M.; Perveen, S.; Kashif, S. M. Synthesis of 4-amino-1,5-dimethyl-2-phenylpyrazolone derivatives and their antioxidant activity. *J. Chem. Soc. Pak.* **2015**, 37, 802–810.
- (18) Qurat-ul-ain; Perveen, S.; Muhammad, M. T.; Yousuf, S.; Khan, K. M.; Choudhary, M. I. Synthetic 4,4'-{(arylmethylene)}bis(1H-pyrazol-5-ols): Efficient radical scavengers. *J. Chem. Soc. Pak.* **2018**, 40, 563–567.
- (19) Ahad, G.; Khan, M.; Khan, A.; Ibrahim, M.; Salar, U.; Kanwal; Khan, K. M.; Perveen, S. Synthesis, structural characterization, and antioxidant activities of 2,4-dinitrophenyl-hydrazone derivatives. *J. Chem. Soc. Pak.* **2018**, 40, 961–973.
- (20) Kohnert, K. D.; Freyse, E. J.; Salzsieder, E. Glycaemic variability and pancreatic β -cell dysfunction. *Curr. Diab. Rev.* **2012**, 8, 345–354.
- (21) Liang, W.; Chen, M.; Zheng, D.; He, J.; Song, M.; Mo, L.; Feng, L.; Lan, J. A novel damage mechanism: Contribution of the interaction between necroptosis and ROS to high glucose-induced injury and inflammation in H9c2 cardiac cells. *Int. J. Mol. Med.* **2017**, 40, 201–208.

- (22) Rosa, M. D.; Distefano, G.; Gagliano, C.; Rusciano, D.; Malaguarnera, L. Autophagy in diabetic retinopathy. *Curr. Neuropharm.* **2016**, *14*, 810–825.
- (23) Epstein, E.; Chen, K. H.; Cohen, J. D. Identification of indole-3-butyric acid as an endogenous constituent of maize kernels and leaves. *Pl. Growth Regul.* **1989**, *8*, 215–223.
- (24) Barden, T. C. *Indoles: Industrial, Agricultural and Over-the-Counter Uses Heterocyclic Scaffolds II: Reactions and applications of Indoles*; Academic Press: Springer, 2010; pp 31–46.
- (25) Shaikh, A. C.; Chen, C. An easy and efficient synthesis of bis-indolyl methanes and tetraindolyl methane Troger's Base catalyzed by AgBF₄. *J. Chin. Chem. Soc.* **2011**, *58*, 899–905.
- (26) Sharma, V.; Kumar, P.; Pathak, D. Biological importance of the indole nucleus in recent years: A comprehensive review. *J. Heterocycl. Chem.* **2010**, *47*, 491–502.
- (27) Liu, X. G.; Li, Z. H.; Xie, J. W.; Liu, P.; Zhang, J.; Dai, B. Copper-catalyzed synthesis of 2,3-disubstituted indoles from *ortho*-haloanilines and β -keto esters/ β -diketone. *Tetrahedron* **2016**, *72*, 653–657.
- (28) Shafakat Ali, N. A.; Ahmad Dar, B.; Pradhan, V.; Farooqui, M. Chemistry and biology of indoles and indazoles: A mini-review. *Mini Rev. Med. Chem.* **2013**, *13*, 1792–1800.
- (29) Radoi, V.; Lixandru, D.; Mohora, M.; Virgolici, B. Advanced glycation end products in diabetes mellitus: mechanism of action and focused treatment. *Proc. Rom. Acad., Ser. B* **2012**, *1*, 9–19.
- (30) Wang, P.; Liu, J.; Xing, H.; Liu, Y.; Xie, W.; Zhao, G. Synthesis and anticancer activity of novel 5-(indole-2-yl)-3-substituted 1,2,4-oxadiazoles. *Drug Discovery Therapy* **2012**, *6*, 133–139.
- (31) Radwan, M. A.; Ragab, E. A.; Sabry, N. M.; El-Shenawy, S. M. Synthesis and biological evaluation of new 3-substituted indole derivatives as potential anti-inflammatory and analgesic agents. *Bioorg. Med. Chem.* **2007**, *15*, 3832–3841.
- (32) Nazir, M.; Abbasi, M. A.; Aziz-ur-Rehman; Siddiqui, S. Z.; Khan, K. M.; Kanwal; Salar, U.; Shahid, M.; Ashraf, M.; Lodhi, M. A.; Khan, F. A. New indole based hybrid oxadiazole scaffolds with *N*-substituted acetamide: As potent anti-diabetic agents. *Bioorg. Chem.* **2018**, *81*, 253–263.
- (33) Taha, M.; Imran, S.; Rahim, F.; Wadood, A.; Khan, K. M. Oxindole based oxadiazole hybrid analogs: Novel α -glucosidase inhibitors. *Bioorg. Chem.* **2018**, *76*, 273–280.
- (34) Taha, M.; Rahim, F.; Imran, S.; Ismail, N. H.; Ullah, H.; Selvaraj, M.; Javid, M. T.; Salar, U.; Ali, M.; Khan, K. M. Synthesis, α -Glucosidase inhibitory activity and *in silico* study of tris-indole hybrid scaffold with oxadiazole ring: As potential leads for the management of type-II diabetes mellitus. *Bioorg. Chem.* **2017**, *74*, 30–40.
- (35) Noreen, T.; Taha, M.; Imran, S.; Chigurupati, S.; Rahim, F.; Selvaraj, M.; Ismail, N. H.; Mohammad, J. I.; Ullah, H.; Javid, M. T.; Nawaz, F.; Irshad, M.; Ali, M. Synthesis of α -amylase inhibitors based on privileged indole scaffold. *Bioorg. Chem.* **2017**, *72*, 248–255.
- (36) Kanwal; Khan, K. M.; Fatima, B.; Bano, B.; Salar, U. A facile route towards the synthesis of 2-(1*H*-indol-3-yl)-acetamides using 1,1-Carbonyldiimidazole. *J. Chem. Soc. Pak.* **2016**, *38*, 771–774.
- (37) Kwon, Y. I.; Apostolidis, E.; Shetty, K. *In vitro* studies of eggplant (*Solanum melongena*) phenolics as inhibitors of key enzymes relevant for type 2 diabetes and hypertension. *Biores. Technol.* **2008**, *99*, 2981–2988.
- (38) Loh, S. P.; Hadira, O. In vitro inhibitory potential of some plants against key enzymes involved in hyperglycemia & hypertension. *Malaysian J. Nutr.* **2011**, *17*, 77–86.
- (39) Chemical Computing Group Inc. Molecular Operating Environment (MOE), 2016.08; 2016.